

Cracks in rubber under tension break the shear wave speed limit

Paul J. Petersan,* Robert D. Deegan, M. Marder, and Harry L. Swinney

Center for Nonlinear Dynamics and Department of Physics,
The University of Texas at Austin, Austin, TX 78712

(Dated: October 26, 2019)

The Rayleigh wave speed has long been thought to be a firm upper limit for the speed of cracks loaded in tension. Here we describe experiments where cracks in tension (Mode I) break this sound barrier, and travel in the intersonic range between shear and longitudinal wave speeds. The experiments are conducted in highly stretched sheets of rubber, and show that intersonic cracks can be produced simply by popping a balloon.

PACS numbers: PACS numbers:62.20.Mk,62.30.+d,81.05.Lg,83.60.Uv

Cracks advance by consuming the potential energy stored in the surrounding elastic fields and, thus, one expects that they should travel no faster than the speed of sound. Solids, however, support longitudinal, shear, and surface (Rayleigh) waves, with distinct speeds $c_L > c_s > c_R$, respectively [1]. Determining which of these speeds limits crack growth poses a surprisingly complex problem.

Stroh was first to argue that cracks loaded in tension (Mode I) could not exceed the Rayleigh wave speed c_R [2]. Careful mathematical analysis [3, 4] shows that the energy consumed by a crack diverges as its speed approaches c_R , suggesting that cracks cannot travel faster than this speed. However, a confluence of geological field measurements of fault motion [5], computer simulations [6, 7], and laboratory experiments [8] established that cracks loaded in shear (Mode II) can exceed c_s (and hence c_R) and reach speeds close to c_L . Dynamic fracture theory was extended to include this phenomenon of “intersonic” cracks [4, 9, 10].

Even when revisited in light of the arguments that allowed intersonic cracks in shear-loaded samples, linear elastic fracture mechanics forbids intersonic cracks loaded in tension [4]. Nevertheless, there is computational and experimental evidence this prohibition is not absolute: Stevenson and Thomas reported unusually fast cracks in rubber loaded in tension, though they did not compare these with sound speeds [11]; and, recently, Buehler and coworkers discovered intersonic Mode I cracks in computer models [12]. Here we present experimental results showing that cracks in biaxially loaded rubber sheets travel at speeds in excess of c_s .

Experiment. Our experiments were conducted with sheets of natural latex rubber 0.15 mm thick purchased from McMaster-Carr, stretched biaxially in a tensile testing machine, and punctured by pricking the sheet with a needle. The samples were rectangular 12.7 cm wide and 27.9 - 34.3 cm long depending on the expected maximum extension, and their perimeter was divided into tabs 3.0 cm wide that served as gripping points for the testing apparatus. A square grid was drawn on the sample to monitor the magnitude and homogeneity of extension

as the sample was stretched.

The apparatus consists of two fixed and two mobile linear guide rails (see Fig. 1(a)). The mobile rails move independently and orthogonally. Multiple sliding clamps that grip individual tabs on the sample are mounted on each rail. The sheet was attached to these clamps and stretched to an extension state (λ_x, λ_y) such that $\lambda_y > \lambda_x$, where λ_i is the ratio of the stretched to original length along the i direction, and x and y are the long and short directions, respectively. As the rails are moved apart, the sheet expands and the clamps separate by sliding along the rail, yet remain equidistant due to the elastic coupling to each other through the sheet.

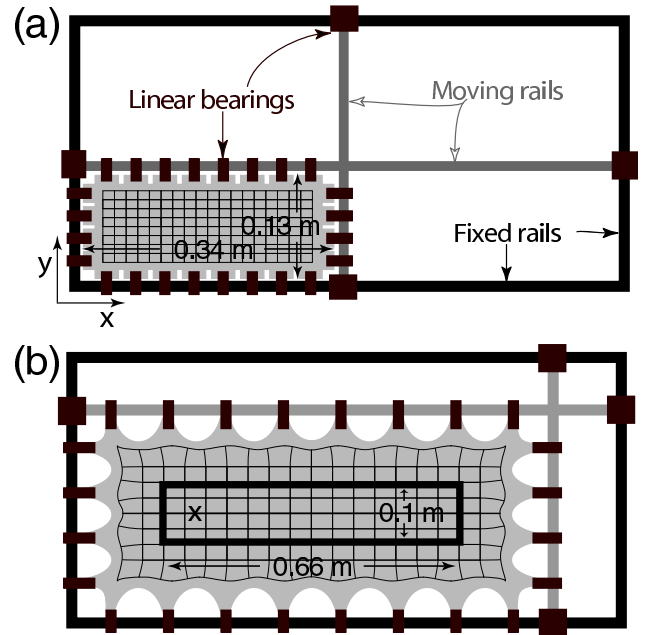


FIG. 1: Apparatus for creating biaxial extensions in a thin rubber sheets. (a) Initial state of the sample loaded in the test apparatus. (b) Final state of the sample after extension. The dark rectangle is a rigid frame attached to the sample and the ‘x’ marks the crack initiation.

After reaching the desired extension state, the sheet is clamped between two steel rectangular frames (10.2 cm ×

66 cm)(Fig. 1(b)). Then the extension state of the sheet is fixed and determined exclusively by these clamping frames. The frames fix the total energy available to the crack, and since the aspect ratio is small, the crack will consume equal amounts of energy per crack length [13].

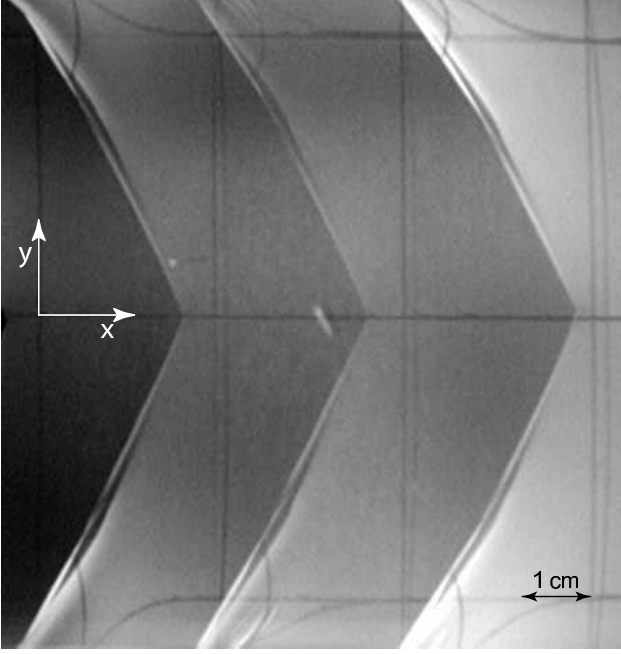


FIG. 2: Multiple exposure photograph of a crack in a rubber sample ($\lambda_x = 2.2$, $\lambda_y = 3.2$). The exposures, separated in time by $500 \mu\text{s}$, are captured on a single frame with a CCD camera.

A crack is initiated by pricking the sheet with a pin at the point marked 'x' in Fig. 1(b) and the velocity is determined photographically. Along the expected crack path we position an optical sensor that triggers a strobing flash when the crack parts the rubber blocking the beam path of the sensor. A CCD camera captures multiple images from each flash pulse on a single frame producing an image as shown in Fig. 2. As reported in [14], the crack can run straight or wavy depending on the extension state; irrespective of the crack path, the velocity of the crack, v_c , is calculated by the distance between successive crack tip positions and the time interval between flashes. Cracks are wavy for $\lambda_x > 2.2$. These measurements are reproducible within 5% from trial to trial.

Longitudinal wave speed. We also measured the longitudinal speed of sound along the x direction in rubber as a function of λ_x and λ_y . In rubber, sound speeds vary strongly with the degree of extension due to the nonlinear strain-extension relation and the large deformations. In particular, when $\lambda_x \neq \lambda_y$, the sound speed depends on the direction. We used a time-of-flight method because standard ultrasonic techniques for measuring sound speeds are difficult to implement. The sheet was first stretched to an extension state $\lambda_y > \lambda_x$. Two record needles

(marked by '+' in Fig. 4(a)) are placed in contact with the sheet about 5 cm apart along the x direction. A bar is attached across the y direction of the sheet about 5 cm from the first needle. The bar is attached to a speaker and an in-plane, x -directed perturbation is applied to the sheet by pulsing the speaker. The signals from the record needles are recorded with a digitizing oscilloscope, and the longitudinal speed in the x direction is calculated from the time lag between the separate signals and the known distance between the needles. Note that the speed is that of a linear wave moving on the stretched material, i.e., we are measuring the propagation speed of infinitesimal distortions around the stretched state.

We were unable to measure the shear wave speed directly due to the thinness of the material which made it difficult to excite shear waves. Instead we measured the appropriate force-extension curve and calculated the velocity from it. As a proof-of-principle, we first calculated in this manner the longitudinal wave speed. We measured the force vs. displacement curve for the configurations depicted in Fig. 4(b). The material was stretched to the state (λ_x, λ_y) , a long but narrow portion was gripped along the long edges, and one of the grips was oscillated sinusoidally at $f = 25 \text{ Hz}$ in the x direction while the other was fixed. A load cell and accelerometer attached to the driven clamp measured the applied force F and acceleration a . The displacement $\delta x = a/(2\pi f)^2$ followed by integration.

Since the measurement is in a strip narrow compared to its length, the strain in the y direction with respect to the *stretched* state ϵ_{yy} is zero almost everywhere. This state of strain correspond to the state excited by a longitudinal wave in a thin sheet: only ϵ_{xx} and ϵ_{zz} are nonzero. Therefore, the force and displacement measurements in this configuration yield the modulus needed to calculate c_L : $Y = FW/(\delta x L d)$ where W is the distance between the grips, L is the length of the grips, d is the thickness of the material in the stretched state, and the longitudinal wave speed along the x direction is $c_L = \sqrt{Y/\rho}$, where $\rho = 944 \text{ kg/m}^3$ is the mass density of the sheet.

The ratio of the measured to calculated wave speed is plotted in Fig. 3 for $\lambda_y = 3.2$ and λ_x varying between 2 and 3.2. The data points lie within experimental error of the value of one, validating the procedure for calculating the wave speed from the force-displacement relationship.

Shear wave speed. With confidence that the procedure yields reliable values, we proceed to calculate the shear wave speed in the x direction. To measure the appropriate shear modulus, a rubber sheet is stretched to $\lambda_y > \lambda_x$, a long and narrow strip of the material is gripped with fixed clamps on opposing sides along the y direction, and a thin bar is glued to the center line between these clamps and oscillated in the direction of the bar (i.e., parallel to the clamps seen in Fig. 4(c)). We measured the force and acceleration on the bar, and calculated the modulus $G = FW/(4\delta x L t)$ and the shear wave speed in the x

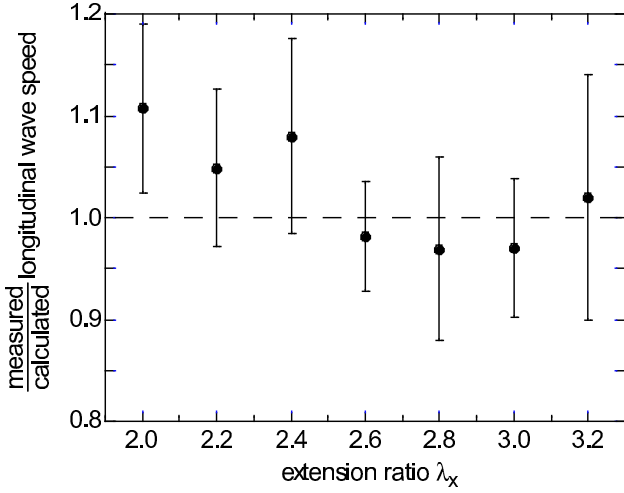


FIG. 3: The ratio of measured to calculated longitudinal wave speed plotted as a function of λ_x for fixed $\lambda_y = 3.2$.

direction, $c_S = \sqrt{G/\rho}$.

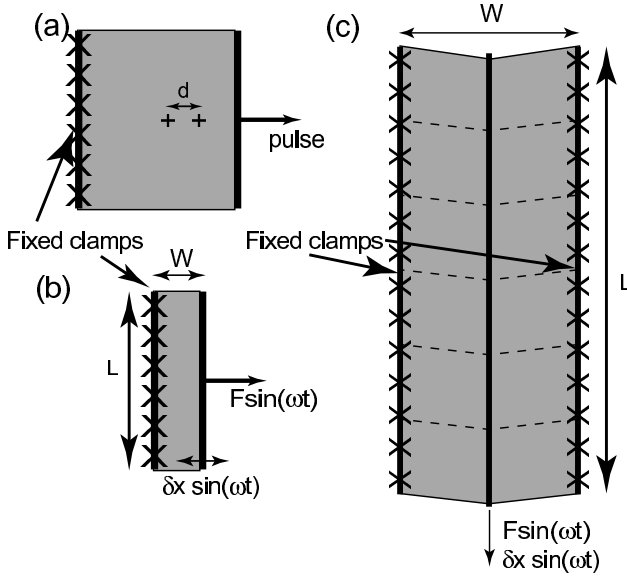


FIG. 4: Experimental configurations for determining sound speeds: (a) direct measurement of the longitudinal wave speed using a time-of-flight method; indirect determination of (b) the longitudinal wave speed and (c) the shear wave speed from a force-displacement measurement. In each setup, the sheet is first brought to the desired state of extension (λ_x, λ_y), the fixed and movable clamps are attached to the sheet, and the measurements proceed.

Material frame. We present our data in the material frame rather than the lab frame because, as we show below, in the material frame wave speeds are isotropic. In the material frame, length is measured in units of a coordinate system that deforms with the material: for biaxial deformation (λ_x, λ_y), the relation between velocity in the material frame $\vec{c}^{(m)}$ and the stretched (or lab)

frame $\vec{c}^{(s)}$ is $\vec{c}^{(m)} = (c_x^{(m)}, c_y^{(m)}) = (c_x^{(s)}/\lambda_x, c_y^{(s)}/\lambda_y)$.

In Fig. 5(a) we compare the longitudinal wave speed in the x and y direction in the material frame for our experimental conditions. As is evident from the data, in the material frame the longitudinal wave speeds in the x and y direction are equal. Thus small deformations and energy transport far ahead of the crack tip are described by isotropic linear elasticity, if one adopts a description in the material frame.

Results. In Figure 5 (b) and (c) we compare crack speeds with wave speeds (far ahead of the crack tip) in the lab and material frame, respectively, as a function of λ_x for $\lambda_y = 3.2$. The data indicate cracks travel 10-20% faster than the shear wave speed, but slower than the longitudinal sound speed. We adopt here the descriptor “intersonic” used in studies of shear loaded cracks, for cracks that travel at speeds between the longitudinal and shear wave speeds.

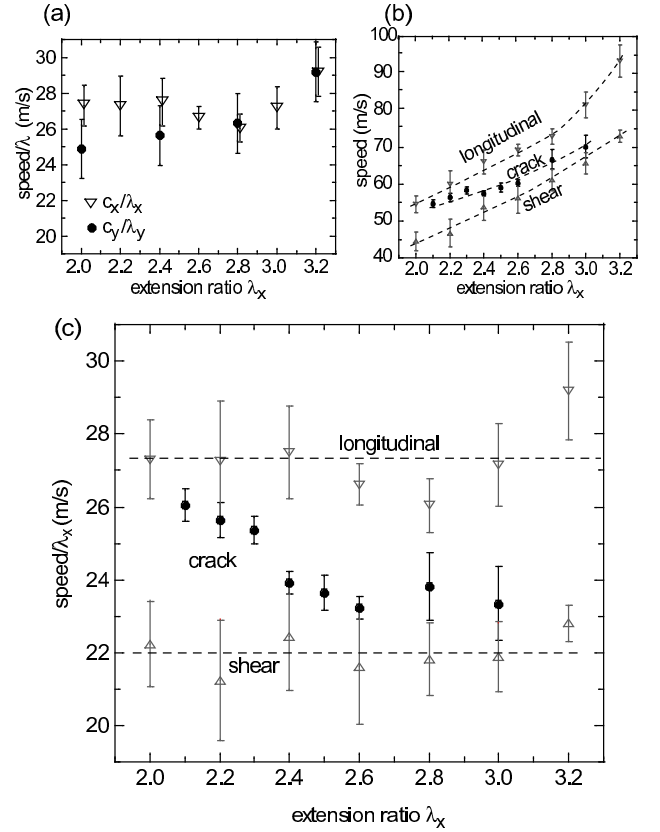


FIG. 5: (a) Comparison between x (∇) and y (\bullet) longitudinal wave speeds in the the material frame as a function of λ_x at fixed $\lambda_y = 3.2$. (b) Crack speed (\bullet), longitudinal wave speed (∇), and shear wave speed (\triangle) as a function of λ_x for $\lambda_y = 3.2$. (c) The same wave and crack speeds in the material frame (dividing through by λ_x). Over the range measured, the shear and longitudinal sound speeds are approximately constant. The dotted lines are guides to the eye.

Theory and simulations. According to linear elastic fracture mechanics the energy flux to the crack tip di-

verges as $v \rightarrow c_R$, and is negative or zero for $v > c_s$ [4]. These results seem to preclude faster-than- c_R tensile cracks: to accelerate past c_R , infinite energy would be needed; even if the crack could jump over this limit, no energy would flow to the tip for $v > c_R$ and, therefore, none would be available to break bonds.

We now try to reconcile our experimental observations with the predictions of continuum mechanics. The seemingly problematic divergence of energy flux to the crack tip is actually not a problem: cracks can change velocity discontinuously [6, 7, 8], i.e., a crack can go from $v < c_R$ to $v > c_s$ without ever passing through c_R .

There is, however, no known loophole within the theory of linear elasticity to reverse the negative energy flux. We propose that the outflow of energy mandated by linear elasticity and the inflow of energy to the crack tip needed to break bonds can be simultaneously satisfied if enough energy is stored in the process zone, the region around the crack tip where linear elasticity ceases to apply [12]. This is possible because of the separation of length scales at which energy is dissipated—the atomic scale—and where linear elasticity is adequate up to $100\text{ }\mu\text{m}$ for polymers depending on the composition [4]. This situation appears to prevail in rubber under typical experimental conditions. The 0.3 MJ/m^2 energy stored per unit cross sectional area far ahead of the crack tip greatly exceeds the 50 J/m^2 [15] needed to pull apart the polymer units near the tip; there is sufficient energy in a $35\text{ }\mu\text{m}$ wide region around the tip for the crack to run.

Furthermore, we have conducted numerical simulations to demonstrate that our scenario is possible at least in principle. In one simulation, 180×60 mass points arranged in a two-dimensional triangular lattice interact via the force law: $F(r) = A(r - r_0)$ for $0 < r < 5r_0$, $F(r) = 4Ar_0$ for $5r_0 < r < 8r_0$, and $F(r) = 0$ for $r > 8r_0$, where r_0 is initial interparticle distance. The sample is stretched to $\lambda_x = 2$ and $\lambda_y = 4.6$; under these conditions, bonds far ahead of the crack tip are stable, but any four vertically angled ones store enough energy to snap a bond. A seed crack is made and allowed to run for $550r_0$ by adding new material ahead of the crack and discarding an equal amount behind it when the crack approached the edge of the sample. The crack speed was $1.4c_s \approx \sqrt{2}c_s$.

According to linear elasticity, no energy flows in or out of the crack tip when a crack loaded in tension travels at $v = \sqrt{2}c_s$ [4], and at intersonic speeds the stress and strain fields vary asymptotically as x^q , where x is the distance to the tip, and q is a speed-dependent exponent equal to zero at $v = \sqrt{2}c_s$. Material displacements are integrals of the strains, so they are described by an ex-

ponent of 1: i.e., the crack opens as $u_y = \pm u_0|x|$, where u_0 is a constant that cannot be determined by these arguments.

Our experiments are only partially consistent with these results. Inspection of Fig. 2 shows that the shape of the crack opening is consistent with the expected wedge shape, and yields $u_0 \approx 0.96$. However, our experiments violate the condition that the crack speed equals $\sqrt{2}c_s$; in fact, we measure that the maximum speed possible, the longitudinal wave speed, is less than $\sqrt{2}c_s$.

In earlier work we found that cracks in rubber follow oscillating paths when the horizontal extension exceeds a critical value. We still have no good explanation for this dynamical transition. However, knowing that the fractures are fed by energy stored just a few microns away from their tips and travel at intersonic speeds will be important in resolving this question.

Acknowledgements—We are grateful for financial support from the National Science Foundation (DMR-9877044 and DMR-0101030). We thank Stephan Bless for lending us the stroboscopic flash that made possible images such as those in Figure 2.

* petersan@chaos.utexas.edu

- [1] J. Achenbach, *Wave Propagation in Elastic Solids* (North Holland, 1973).
- [2] A. Stroh, *Philosophical Magazine* **6**, 418 (1957), supplement: Advances in Physics.
- [3] L. B. Freund, *Dynamic Fracture Mechanics* (Cambridge University Press, Cambridge, 1990).
- [4] K. B. Broberg, *Cracks and Fracture* (Academic Press, San Diego, 1999), ISBN 0-12-134130-5.
- [5] T. H. Heaton, *Phys. Earth Planet. Interiors* **64**, 1 (1990).
- [6] D. J. Andrews, *Journal of Geophysical Research* **81**, 5679 (1976).
- [7] H. Gao, Y. Huang, and F. F. Abraham, *JMPS* **49**, 2113 (2001).
- [8] A. J. Rosakis, *Advances in Physics* **51**, 1189 (2002).
- [9] R. Burridge, G. Conn, and L. Freund, *J. Geophys. Res.* **84**, 2210 (1979).
- [10] K. Ranjith and J. R. Rice, *Journal of the Mechanics and Physics of Solids* **49**, 341 (2001).
- [11] A. Stevenson and A. Thomas, *J. Phys. D: Appl. Phys.* **12**, 2101 (1979).
- [12] M. J. Buehler, F. F. Abraham, and H. Gao, *Nature* **426**, 141 (2003).
- [13] J. R. Rice, *Journal of Applied Mechanics* **34**, 248 (1967).
- [14] R. D. Deegan, P. J. Petersan, M. Marder, and H. L. Swinney, *Phys. Rev. Lett.* **88**, 014304 (2002).
- [15] A. Thomas, *Rubber Chem. Tech.* **67**, G50 (1994).